International Journal of Nanomedicine

Dovepress

open access to scientific and medical research

Open Access Full Text Article

ORIGINAL RESEARCH

Cellular Uptake of Silica Particles Influences EGFR Signaling Pathway and is Affected in Response to EGF

Mauro Sousa de Almeida[1], Arya Roshanfekr[1], Sandor Balog[1], Alke Petri-Fink[1,2], Barbara Rothen-Rutishauser[1]

[1]Adolphe Merkle Institute, University of Fribourg, Fribourg, Switzerland; [2]Department of Chemistry, University of Fribourg, Fribourg, Switzerland

Correspondence: Barbara Rothen-Rutishauser, Adolphe Merkle Institute, University of Fribourg, Fribourg, Switzerland, Email barbara.rothen@unifr.ch

Background: The human epidermal growth factor receptor (EGFR) is a receptor tyrosine kinase that is involved in several key cellular processes, such as cell proliferation and differentiation, and it has been linked to the development and progression of various cancers (e.g., breast and lung). Researchers have attempted to improve current cancer-targeted therapies by conjugating molecules on the surface of (nano)particles to efficiently target and inhibit EGFR. However, very few in vitro studies have investigated the effect of particles per se on EGFR signaling and dynamics. Furthermore, the impact of concomitant exposure of particles and EGFR ligands, such as epidermal growth factor (EGF) on cellular uptake efficiency has received little attention.

Purpose: The purpose of this research was to determine the effects of silica (SiO_2) particles on EGFR expression and intracellular signaling pathways in A549 lung epithelial cells, in the presence or absence of epidermal growth factor (EGF).

Results: We showed that A549 cells are able to internalize SiO_2 particles with core diameters of 130 nm and 1 μm without affecting cell proliferation or migration. However, both SiO_2 particles interfere with the EGFR signaling pathway by raising the endogenous levels of extracellular signal-regulated kinase (ERK) 1/2. Furthermore, both in the presence and absence of SiO_2 particles, the addition of EGF increased cell migration. EGF also stimulated cellular uptake of 130 nm SiO_2 particles but not 1 μm particles. The increased uptake is primarily associated with EGF-stimulated macropinocytosis.

Conclusion: This study shows that SiO_2 particle uptake interferes with cellular signaling pathways and can be boosted by concurrent exposure to the bioactive molecule EGF. SiO_2 particles, both alone and in combination with the ligand EGF, interfere with EGFR signaling pathway in a size-dependent manner.

Keywords: endocytosis, nanoparticles, epidermal growth factor, cellular signaling

Introduction

Human epidermal growth factor (EGF) is a small protein capable of inducing cell growth and differentiation upon binding to EGF receptor (EGFR).[1] EGF can be found in varying concentrations in the human body. Plasma, serum, and saliva have low EGF concentrations (1–2 ng/mL), whereas bile and urine have much higher concentrations (50–500 ng/mL).[2] At low EGF concentrations (i.e., <10 ng/mL), EGF binds to EGFR and the ligand-receptor complex is mainly internalized through clathrin-mediated endocytosis, however, at relative high doses of EGF (i.e., ≥10 ng/mL), clathrin-independent endocytosis also takes place.[3] The transmembrane protein EGFR is a member of the ErbB family of receptor tyrosine kinases (RTK). This receptor regulates various important cellular processes, such as cell proliferation, migration, differentiation, survival and oncogenesis.[2,4] There are seven different ligands/growth factors able to bind and activate EGFR. They can be divided into two different groups: high-affinity ligands (EGF, transforming growth factor-α (TGFα), beta-cellulin (BTC), and heparin binding EGF-like growth factor (HB-EGF)) and low-affinity ligands (epiregulin (EREG), epigen (EPGN), and amphiregulin (AREG)).[5] The different ligands bind and activate EGFR in a similar manner. EGFR signaling is initiated upon ligand–receptor interaction, leading to receptor dimerization and phosphorylation of tyrosine residues in the cytoplasmic tail.[6] EGFR autophosphorylation recruits adaptor and signaling proteins, which then trigger several downstream signaling pathways, such as the PI3K/Akt/PTEN/mTOR and RAS/RAF/MEK/ERK.[6,7]

Received: 15 September 2022
Accepted: 3 February 2023
Published: 24 February 2023

EGFR is known to be upregulated in cells under several pathological conditions, such as lung and breast cancer, and glioblastoma.[8] EGFR overexpression correlates with increased in vivo tumor invasiveness and in vitro cell migration.[9] Cell migration is a critical step in tumor cell metastasis, and EGF is thought to be a key chemoattractant in breast cancer invasion.[10,11] In this direction, a significant research has been carried out in the past 20 years on the development of nanocarriers, such as nanoparticles (NPs), to target and inhibit EGFR.[12] NPs are appealing for medical applications due to their unique characteristics, such as the larger surface-to-mass ratio compared to other particles, and their ability to bind and carry other molecules.[13] They improve drug transport across cell membranes and prolong blood circulation times.[14] Their surface area allows the binding and transport of drugs and proteins.[15] Surface functionalization of NPs with protein ligands (e.g., EGF) capable of binding to their receptors (e.g., EGFR) is an NP targeting strategy used to increase NP delivery into specific cells. Due to the FDA approval of antibody immunotherapies, such as trastuzumab and cetuximab, the majority of current research focuses on the functionalization of NPs with antibodies and antibody fragments to target EGFR.[16] Nevertheless, other approaches such as NP functionalization with the native ligand EGF, specific aptamers, and low molecular weight peptides have also emerged. For example, Silva et al have functionalized hyaluronic acid-oleic acid (HAOA) coated gold NPs with EGF.[17] The functionalized spherical NPs (100−200 nm) demonstrated a potential application for near-infrared (NIR, 650–800 nm) photothermal therapy as well as high biocompatibility with healthy tissues and the ability to be internalized by the EGFR-overexpressing adenocarcinoma lung epithelial cell-line A549 via different mechanisms. In another study, She et al showed that the target efficiency of EGF grafted on spherical mesoporous silica NPs (~100 nm) in colorectal cancer SW 480 cells was affected by the number of EGFs attached onto the NP's surface.[18]

Despite expending a significant effort to efficiently target cancer cells using particle functionalization strategies, a large portion of those appears to fail due to a loss of targeting ability after interaction with biological fluids and active biomolecules that can adsorb onto the NP's surface (i.e., protein corona).[19,20] The enhanced uptake and accumulation of NPs in target cells is essential for achieving high treatment efficacy. This can be achieved by NP surface functionalization, as previously mentioned, but also by combined therapy where NPs can be administered together with other molecules that are able to stimulate NP uptake.[21,22] Phuc et al have shown that EGF at 100 ng/mL enhances the uptake of spherical polystyrene NPs (50 nm) in human epidermoid carcinoma-derived A431 cells.[23] Nevertheless, the effect of NPs per se on the EGFR dynamics, including signaling and recycling has not been thoroughly investigated.

Based on the idea that NPs can interfere with different signaling pathways and that NPs co-exposure with bioactive molecules, such as EGF, can influence NP uptake, we decided to investigate the impact of different sized silica (SiO_2) particles uptake on the expression and dynamics of EGFR in A549 cells, in the presence or absence of EGF. In addition, a cell migration assay was performed to study if particles in the presence or absence of EGF interfere with cell migration.

Materials and Methods

Synthesis and Characterization of SiO_2-Cy5 Particles

Synthesis of SiO_2 particles labeled with the fluorescent dye cyanine 5 (Cy5) was performed following a modified Stöber method.[24,25] For the synthesis of ~130 nm SiO_2 particles, 29 mL H_2O, 81 mL ethanol (>99.8%, analytical grade, VWR, Dietikon, Switzerland) and 2.9 mL of ammonia solution (25% for analysis, Merck, Zug, Switzerland) were magnetically stirred for 30 min in a round-bottom flask equipped with a reflux system at 60°C. Then, 10 mL of tetraethylorthosilicate (TEOS) (>99.0%, Sigma Aldrich, Germany) was added and stirred for two minutes after which 200 µL of a mixture containing 2.3 mg of sulfo-Cy5 NHS ester (Lumiprobe, Germany) and 3 µL of (3-aminopropyl)triethoxysilane (APTES) (99%, Sigma Aldrich, Germany) in dimethylsiloxane (DMSO) (>99.9%, sterile-filtered, Sigma Aldrich, Germany) was added and the solution was allowed to react for 5 h. The obtained particles were isolated by several cycles of centrifugation (three times at 2000 g for 40 min) and redispersion in Milli-Q water.

Micron-sized particles (~1 µm) were prepared in a similar manner with slight modifications. In a polystyrene bottle, 12.9 mL of Milli-Q water, 14.7 mL of EtOH, and 16 mL of ammonia were mixed with a stir bar and heated to 40 °C. Thirty minutes later, 8.4 mL of TEOS was added fast and the mixture was allowed to run for 15 min, leading to the formation of particles with a hydrodynamic diameter of roughly 500 nm. The particle dispersion

was then transferred to a 500 mL plastic bottle and heated at 40 °C while being stirred magnetically (900 rpm). Then, 22.38 mL of water, 8.43 mL of EtOH, and 2.15 mL of ammonia were added to the solution for 10 min, followed by the addition of 16 mL of TEOS for 15 min. To obtain particles in the size range of ~1 µm, this step was repeated three more times and 2 min after the fourth addition, 300 µL of a solution containing 1.15 mg of sulfo-Cy5 NHS ester and 3.9 µL of APTES in DMSO was added to the reaction. The solution was heated at 40°C for 45 min, and to remove the excess of unbound Cy5, the particle dispersion was centrifuged two times at 1000 rpm for 15 min. Both particles (~130 nm and ~1 µm) were redispersed in Milli-Q water before being stored in fridge.

Particle size distribution was calculated with a particle size analysis (ImageJ, National Institutes of Health, Bethesda, MD, USA), based on images taken with a transmission electron microscope (TEM, FEI Tecnai G2 Filter, Hillsboro, OR, US). The stability of both particles in the cell culture media was tested at 24 h by dynamic light scattering (DLS) at 90° with a commercial goniometer instrument (3D LS Spectrometer, LS Instruments AG, Switzerland) fitted with a linearly polarized and a collimated laser beam (Cobolt 05-01 diode-pumped solid-state laser) working at a fixed wavelength of 660 nm, as previously described.[26,27] At least five independent measurements were performed and, as a control condition, particle suspension in water was measured. The phase-amplitude light scattering technique (ZetaPALS, Brookhaven Instruments Corp., USA) was used to determine the zeta potential of particles suspended in water.

Cell Culture

Unless otherwise stated, all materials for cell culture were bought from Gibco, Thermo Fisher Scientific (Switzerland). Human alveolar epithelial type II cells (A549 cell line) from American Tissue Type Culture Collection (ATCC) and A549 with GFP-tagged EGFR (GFP-EGFR) from Sigma Aldrich, Switzerland, were cultured at 37°C, in 5% CO_2 and 95% humidity and passaged twice per week, at 80–90% cell confluence. Both cells were maintained in Roswell Park Memorial Institute (RPMI)-1640 cell culture media supplemented with 10% fetal bovine serum (FBS), 2 mM L-Glutamine, 100 U/mL penicillin, and 100 µg/mL streptomycin. The final solution of RPMI-1640 is further mentioned as complete RPMI (cRPMI).

Cell Exposure to EGF and Particles

A549 and A549 GFP-EGFR cells (passage 4–22) were seeded in different cell culture dishes (see next sections) until they reached 80–100% confluence. Serum deprivation for 24 hours prior to exposure to EGF and particles were used to synchronize cell cycle. Then the cells were exposed to 100 ng/mL human EGF (Cat.# 130-097-749, Miltenyi Biotec, Germany) and/or 130 nm SiO_2-Cy5 particles, and/or 1 µm SiO_2-Cy5 particles ([NP] = 50 µg/mL) previously suspended in cRPMI.

Cell Viability Assay

The WST-1 assay (Roche Diagnostics, Mannheim, Germany) was used to measure the mitochondrial activity and respective cell viability. A549 cells were seeded in 96-well plates (1 x 10^4 cells/well) for 24 h in cRPMI and exposed to EGF and particles for 24 h and 48 h. Then, cells were washed three times before being exposed to 100 µL of WST-1 solution diluted 1:10 in cRPMI for at least 30 min. Absorbance was measured at a wavelength of 450 nm. All tests were performed in triplicate. Interference analysis was performed for SiO_2 particles at 50 µg/mL, in one biological experiment and three technical replicates. There was no sign of quenching or auto-absorption (Figure S1).

Cytotoxicity Assay

After each exposure, the cell supernatant was collected and a lactate dehydrogenase (LDH, Roche Applied Science, Mannheim, Germany) assay was performed. As a positive control, 0.2 vol.% Triton X-100 was added to the cell culture medium 24 h before collecting the supernatant. Samples were measured in triplicate. The final product absorbance was measured with a spectrophotometer at 490 nm with a reference wavelength of 630 nm (Benchmark Microplate reader, BioRad, Cressier, Switzerland).

Cell Migration Assay

A549 cells were seeded into 24-well plates (1×10^5 cells/well) and grown for 48 h until they reached confluence. A "scratch/wound" was created by scraping the cell monolayer with a p200 pipette tip in a straight line. Two washing steps with cRPMI were performed in order to remove cell debris. Cells were then exposed to 0.5 mL of EGF and/or particles for 24 h. Micrographs of the wound were taken at 0 h, 6 h and 24 h using a phase-contrast light microscope (Motic AE2000, Wetzlar, Germany). The area of the wound at 6 h and 24 h was determined with ImageJ and normalized against the wound area at 0 h.

Flow Cytometry

A549 cells grown in 12-well plates (1×10^5 cells/well) were exposed to 1 mL EGF, particles and FITC-dextran (70 kDa, 0.25 mg/mL, Cat.# 46945, Sigma-Aldrich, Switzerland) previously suspended in cRPMI, for 6 h and 24 h. Cells were pre-treated with the macropinocytosis inhibitor, 5-(N-ethyl-N-isopropyl)amiloride (EIPA, 50 µM, Cat.# 3378, R&D, UK), for 1 h at 37 °C in serum-free cell culture media before being treated with EGF, particles, and dextran in cRPMI-containing EIPA for 6 h. Cells were detached with 100 µL of Trypsin-Ethylenediaminetetraacetic acid (EDTA) for 6 min and 900 µL of cRPMI was added. Then, a centrifugation step was performed for 5 min at 300 g and 4°C, followed by cell washing with phosphate-buffered saline solution (PBS, pH 7.2, Gibco, Life Technologies Europe B.V., Zug, Switzerland). Finally, cells were resuspended in cold flow cytometry buffer (PBS containing 1 w/v% bovine serum albumin (BSA, Sigma-Aldrich, Switzerland), 0.1 vol.% sodium azide (Sigma-Aldrich, Switzerland) and 1 mM EDTA (Sigma-Aldrich, Switzerland) at pH 7.4. Data acquisition was carried out on a BD LSR FORTESSA (BD Biosciences, USA) fitted with a red laser and APC filter where 30,000 events were processed. The FlowJo program v.10.7.1 was used to analyze the data.

Fluorescence Imaging

A549 GFP-EGFR cells (4×10^4 cells/well) were seeded into µ-Slide 8 Wells (Ibidi, Germany). Cells were then exposed to EGF and/or particles for 6 h and 24 h, and fixed with 4 vol.% PFA in PBS for 15 min. Then, cells were permeabilized with 0.2 vol.% Triton X-100 in PBS for 10 min and washed thrice with PBS. Samples were maintained in PBS until further analysis. All procedure was conducted in the dark and at room temperature. Image acquisition was carried out in an inverted confocal system (Leica, Stellaris 5, Germany), equipped with Power HyD S detectors, a Plan-Apochromat 63x/1.4 Oil CS2 objective (Leica, Switzerland) and controlled by LAS X (Leica). Three different excitations laser were used: 405 nm (DAPI), 488 nm (GFP), and 633 nm (Cy5).

Colocalization Analysis

Colocalization of the exposed particles with lysosomes and EGFR was evaluated after 6 h and 24 h. Following exposure to EGF/particles, cells were washed three times with PBS before staining with a solution containing 100 nM LysoTracker Blue DND-22 (Invitrogen, Thermo Fisher Scientific Inc., Switzerland) in cRPMI for 30 min. Before cell imaging, samples were washed twice with PBS and phenol-free cRPMI was added. Z-stacks were acquired sequentially, collected with a field of view of 144.80 µm x 144.80 µm with a pixel density of 1880 × 1880 and a pixel dwell time of 0.31 µs. Data are shown as mean + standard error of the mean for n = 10 cells. The Pearson's correlation coefficient (PCC) was determined using EzColocalization (Image J plugin).[28]

Western Blot

The Western blot was performed as previously reported with slight modifications.[29] After cell treatment with EGF/particles in 12-well plates, cell lysis was carried out to isolate the total protein. Cells were washed two times with PBS before adding 80 µL of ice-cold M-PER buffer (Cat. # 78501, Thermo Scientific) supplemented with Halt™ Protease Inhibitor Cocktail, EDTA-free (Cat. # 78425, Thermo Scientific). Plates were kept in the fridge for 15 min to ensure an efficient lysis, after which the cell lysates were pipetted up and down five times and transferred into Eppendorf tubes. The samples were placed on ice for at least 10 min before being centrifuged for 5 min at 14,000 g. The supernatant containing proteins was collected and protein concentration was measured spectrophotometrically (NanoDrop™ 2000

Spectrophotometer, Thermo Scientific) at the wavelength of 280 nm. The samples were heated for 5 min at 90°C in a reducing Laemmli buffer, before loading the same amount of protein in a 7.5% and 12.5% SDS-PAGE (Bio-Rad, Hercules, CA, USA). A wet transfer of proteins from the gel to polyvinylidene difluoride (PVDF) membranes was performed for 75 min at 150 mA. To visualize the transferred proteins, the membrane was stained with a solution containing 0.1 w/v.% Ponceau S (Cat. # 141194, Sigma-Aldrich, Switzerland). A blocking solution containing 4 w/v.% BSA and 0.1 vol.% Tween 20 (Cat. # P9416, Sigma-Aldrich, Switzerland) in Tris-buffered saline (TBS) was added to the membrane for 1 h. Immunostaining was carried out using the same solution. Between steps, three washes with TBST (0.1 vol.% Tween 20 in TBS) were performed. Primary antibodies against EGFR (1 µg/mL, Cat. # AF231, R&D, UK), p-ERK1/2 (1 µg/mL, Cat. # sc-7383, Santa Cruz Technology, USA), GAPDH (1 µg/mL, sc-47724, Santa Cruz Technology, USA) and α-tubulin (1 µg/mL, Cat. # sc-32293, Santa Cruz Technology, USA) were added to the blots overnight at 4°C. Then, a secondary antibody goat anti-mouse horseradish peroxidase (HRP) (Cat. # HAF007, R&D, UK) at 1:2000 (α-tubulin), 1:4000 (GAPDH), 1:1000 (EGFR), 1:1000 (ERK1/2 and p-ERK1/2) was added to the membranes for 1 h. A protein standard (mPAGE® Color Protein Standard, Cat. # MPSTD4, Sigma-Aldrich, Switzerland) was used to confirm the molecular weight of the detected bands. The chemiluminescence detection of the protein bands was performed with an HRP substrate (Immobilon Forte Western HRP substrate, Cat. # WBLUF0020, Sigma-Aldrich, Switzerland). The detection of total ERK1/2 was performed after mild stripping of the p-ERK1/2. After p-ERK1/2 detection, membrane was washed twice with TBST. The membrane was covered with a mild stripping buffer containing 5 w/v % glycine (Sigma-Aldrich, Switzerland), 0.1 w/v % SDS (Sigma-Aldrich, Switzerland), 1 vol.% Tween-20 in Milli-Q water at pH 2.8 for 10 min. The buffer was discarded, and new buffer was added for 10 min. A round of washing with TBS and two washing rounds with TBST were performed. Blocking, immunostaining, and visualization steps were carried out as previously mentioned, with a slight difference for primary antibody staining. Anti-ERK1/2 (1 µg/mL, Cat. # sc-514302, Santa Cruz Technology, USA) was only added to the blot for 1 h at room temperature. The semi-quantification of proteins was performed by measuring the optical density of the bands with ImageJ. To normalize the data, two housekeeping proteins α-tubulin and GAPDH were used.

Statistical Analyses

Unpaired *t*-test was used to compare two independent groups, while paired *t*-test was used to compare two related groups. The comparison between more than two groups with one variable was performed with one way ANOVA (Tukey's and Dunnett's post-hoc test for multiple comparisons). Statistical analyses were performed with GraphPad Prism 9.2 software (GraphPad Software).

Results and Discussion

SiO_2–Cy5 Particles Characterization and Uptake by Lung Epithelial Cells

Herein, two fluorescently labelled spherical SiO_2-Cy5 particles with diameter sizes of ~130 nm and 1 µm were synthesized to investigate the effect of particle size on the cellular uptake and EGFR signaling and dynamics. The fluorescent dye Cy5 was incorporated into the particles during the synthesis to enable particle detection within cells using confocal laser scanning microscopy (cLSM) and flow cytometry. Physical properties of both particles, such as size and shape were assessed using transmission electron microscopy (TEM) and image analysis (Figure 1A–D). Hydrodynamic diameter and zeta potential were determined in Milli-Q water by DLS and PALS, respectively (Figure 1E inset table and Figure S2). Analysis of TEM micrographs revealed spherical particles with core diameters of 135 nm and 980 nm, while DLS measurements revealed particles with hydrodynamic diameters of 130 nm and 1280 nm. Nevertheless, particle stability can be affected in different media, such as cell culture medium. The presence of salts and macromolecules in cell culture medium can impact particle colloidal stability.[30] As previously demonstrated, the interaction of NPs with mammalian cells, as individual particles, with or without protein corona, or in an aggregated state, can lead to different uptake and/or different cellular responses.[27,30] Particle aggregation occurs when single NPs cluster together, resulting in an increase in size, which directly interferes with the cellular internalization mechanism. Therefore, DLS measurements were employed to evaluate the stability of both SiO_2 particles in cRPMI at 24 h, with no significant changes in

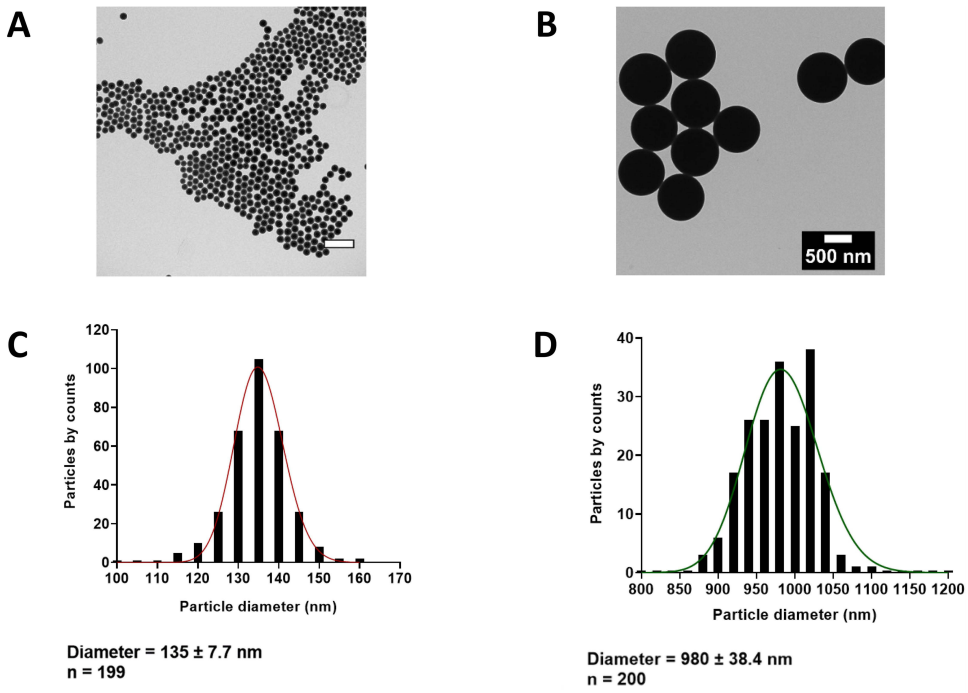

E

Particles	Hydrodynamic diameter (D_H)	
	H_20	Complete RPMI 1640
SiO_2-Cy5 130 nm	132.4 ± 12.6 nm	167.2 ± 40.0 nm
SiO_2-Cy5 1 µm	1278.2 ± 447.2 nm	1343.6 ± 545.6 nm

Figure 1 Physicochemical properties of SiO_2 particles and stability in cell culture medium. Representative transmission electron microscopy (TEM) micrographs of 130 nm and 1 µm SiO_2-Cy5 particles (**A** and **B**) in H_20 and corresponding histograms showing the particle size distribution (**C** and **D**). Scale bar = 500 nm. (**E**) Hydrodynamic diameter determined by dynamic light scattering in H_2O and complete RPMI 1640 (cRPMI) revealing the stability of both particles in cRPMI.

hydrodynamic diameter. We have previously demonstrated that SiO_2 NPs are stable in cRPMI, but they tend to aggregate in serum-free RPMI.[29] Cell experiments were carried out in cRPMI due to aggregation of SiO_2 NPs in serum-free RPMI. Zeta potential measurements of particle dispersions in water showed strong negative zeta potential values (<−30 mV) indicating a stable particle suspension.

The human adenocarcinomic lung epithelial cell (A549) line was selected for this study because it is a commonly used cell line to mimic an alveolar type II epithelial tissue and to investigate cell–particle interactions.[31,32] Previous research has proved that silica particles are able to stimulate the proliferation of human adipose tissue-derived stem cells (hADSCs) and human gastric carcinoma cells.[33,34] To investigate the effect of EGF and SiO_2 particles on mitochondrial activity of A549 cells, a WST-1 assay was employed at two different time points (24 h and 48 h). A condition in which cells were kept in serum-free medium was included to compare the impact of serum on mitochondrial activity. Cells grown in serum-free medium exhibited a low percentage of mitochondrial activity (Figure S3A and B). At 24 h, the larger SiO_2 particles slightly increased the mitochondrial activity of A549 cells, but this effect is not statistically significant. The results reveal that EGF and SiO_2 particles had no significant effect on the mitochondrial activity of A549 cells.

In addition, a lactate dehydrogenase assay was performed to evaluate the cellular cytotoxicity of EGF and SiO_2 NPs after 24 h exposure (Figure S3A–C). No major differences in cell membrane permeability after exposure were observed, confirming non-cytotoxicity effects.

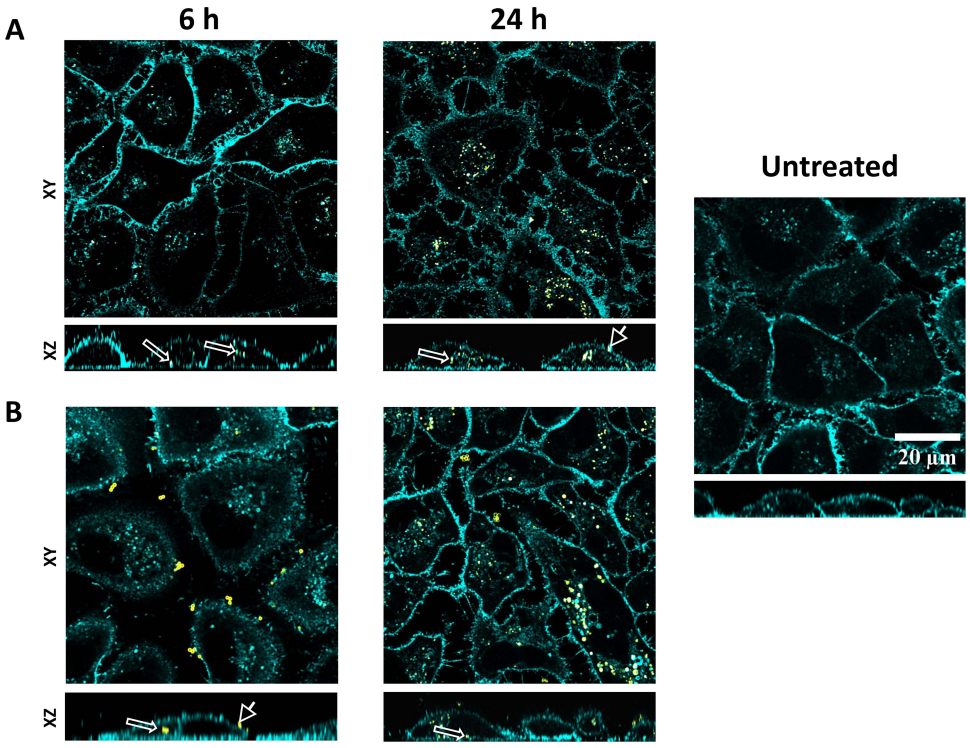

Figure 2 Cellular uptake of SiO_2 particles. Confocal laser scanning microscopy (cLSM) showing the interaction and internalization of 130 nm (**A**) and 1 µm (**B**) SiO_2 particles within lung epithelial cells (A549) after 6 and 24 h of exposure. Scale bar = 20 µm. Particles in yellow and EGFR-GFP in cyan. Arrows and arrowheads indicate intracellular and extracellular particles, respectively.

Then, we investigated cell–particle interaction through cLSM at 6 h and 24 h (Figure 2). We observed that both 130 nm and 1 µm particles were internalized by A549 cells upon 6 h exposure. Nonetheless, a significant number of large particles can be seen in contact with the outer cell membrane but are not internalized. The intracellular signal for both particles increased at 24 h, indicating that particle uptake increased overtime. Smaller particles are expected to be internalized via different endocytic mechanisms, such as clathrin-mediated endocytosis and macropinocytosis, whereas larger particles are mainly internalized via macropinocytosis.[21]

Influence of Epidermal Growth Factor on the Uptake and Intracellular Localization of SiO_2 Particles in Lung Epithelial Cells

After observing that particle internalization occurs within the first 6 h and that SiO_2 particles and EGF do not interfere with mitochondrial activity or membrane permeability, we decided to investigate the influence of EGF treatment on SiO_2 particle uptake by cells. To analyze cell-particle association flow cytometry was performed (Figure 3). The term particle association refers to both cell membrane-bound and internalized particles. The association of 130 nm SiO_2 particles with A549 cells was increased at 6 h (28%) and 24 h (29%) in the presence of EGF (100 ng/mL). This trend was not seen for larger SiO_2 particles at 6 h. However, at 24 h time point, a slight but not statistically significant increase of 14% on median fluorescence intensity (MFI) values was observed for EGF and 1 µm SiO_2 particles. The same outcome can be seen in cLSM maximum projection intensity images (Figure S4). The intensity signal for 130 nm SiO_2 particles increases after 24 h in the presence of EGF. The effect of EGF on the macropinocytosis marker (i.e., dextran) uptake was also evaluated. An increase of 52% (6 h) and 48% (24 h) on MFI values occurred when EGF was added concomitantly with dextran. Additional experiments with the macropinocytosis inhibitor EIPA were carried out to determine the involvement of this endocytic mechanism. EIPA treatment for 6 h reduced the association of both particles with A549 cells. Furthermore, EIPA inhibited the potentiating EGF effect on cell-130 nm SiO_2 particles association. The results clearly show that EGF stimulates the association of smaller particles and dextran with A549 cells in the first 6 h, but this behavior is not observed for larger particles. The increase in

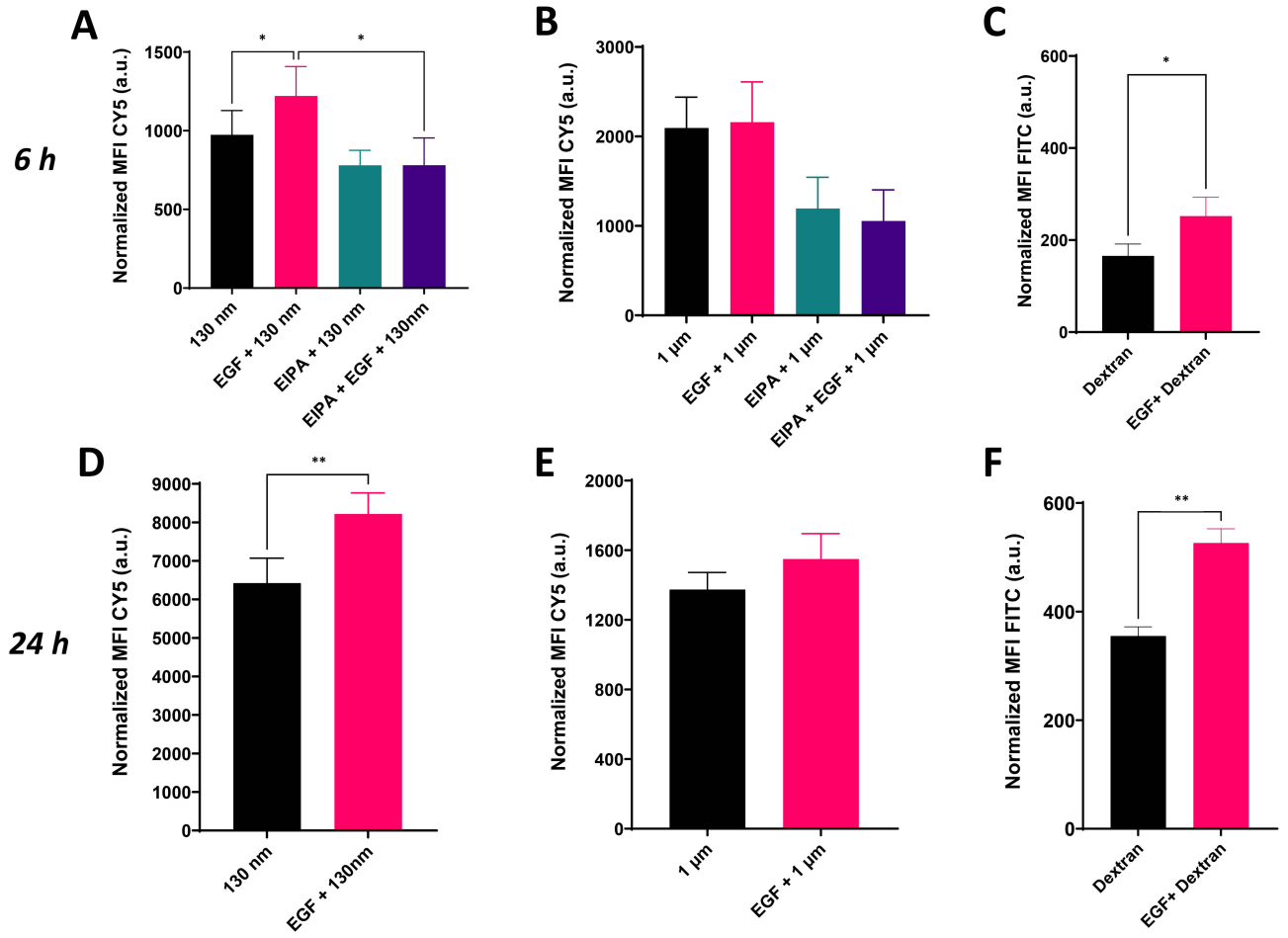

Figure 3 Effect of epidermal growth factor (100 ng/mL) on the cellular uptake of SiO_2 particles and dextran at different time points. Bar graphs show the median fluorescence intensity (MFI) values obtained from flow cytometry measurements upon 6 h (**A**–**C**) and 24 h exposure (**D**–**F**) of lung epithelial cells (A549) to 50 µg/mL SiO_2 particles (**A, B, D** and **E**), 50 µM EIPA (**A** and **B**) and 250 µg/mL dextran (**C** and **F**). Data are presented as mean ± standard error of mean (n = 3). Statistically significant differences among the groups (One-way ANOVA Tukey's post-hoc test for multiple comparisons (**A** and **B**) and paired *t*-test (**C**–**F**)): *p ≤ 0.05; **p ≤ 0.01.

dextran uptake and decrease of particle uptake in the presence of EIPA, indicates that EGF potentiates macropinocytosis of 130 nm SiO_2 particles. Considering that macropinocytosis is increased and that macropinosomes possess a size range between 0.2 and 3 µm, an increase on the uptake of 1 µm SiO_2 particles was also expected. Nonetheless, we only observed a slight but not statistically significant increase in the association of these particles with A549 after 24 h. It has been reported that large particles (>500 nm) are only internalized via phagocytosis and/or macropinocytosis.[21,35] Other endocytic mechanisms, such as clathrin-mediated and caveolae-dependent endocytosis, are cargo size limited (200–300 nm).[36,37] According to this, macropinocytosis is the primary mechanism by which A549 cells internalize 1 µm SiO_2 particles. However, we believe that one of the main explanations for this finding is the formation of macropinosomes in response to EGF stimulation, which are probably too small to wrap the larger particles (<1 µm). The enhancement of particle uptake upon EGF stimulation has been also shown by Phuc et al,[23] where they proved that EGF, at 100 ng/mL, is capable of enhancing the uptake of spherical 50 nm polystyrene NPs (50 nm) in human epidermoid carcinoma-derived A431 cells. Similarly to NPs, Nakase et al demonstrated the ability of EGF (500 nM) to stimulate macropinocytosis and potentiate exosome (~100 nm) uptake in three different cell lines (human pancreas carcinoma-derived MIA PaCa-2 cells, human pancreas adenocarcinoma-derived BxPC-3 cells, and A431 cells).[38] Even if EGF-stimulated macropinocytosis is one of the main explanations for the higher association of 130 nm SiO_2 particles with A549 cells, EGF stimulation of other endocytic mechanisms should also be considered. At high EGF concentrations (i.e., <10 ng/mL) clathrin-mediated and clathrin-independent endocytosis are activated, which can also explain the increase on the uptake of smaller SiO_2 particles.[3] The

activation of these mechanisms might facilitate the internalization of smaller particles, but not the larger ones due to the size-dependency of the vesicles formed (<300 nm).

When particles deposit on the outer cell membrane, they can be wrapped by the membrane and end up inside endocytic vesicles, which travel along microtubules in the cell cytoplasm, fusing with early endosomes and, later, with lysosomes.[21] With this in mind, colocalization of SiO_2 particles with lysosomes was investigated. Lysotracker, a fluorescent dye, was used for labeling and tracking lysosomes. Two time points were chosen based on the assumption that particles require some time to be internalized and transported intracellularly (6 h and 24 h). At 6 h, our results (Figure 4A and B) show a very low colocalization (Pearson correlation coefficient (PCC) < 0.3) between the particles and lysotracker. Higher colocalization values for both particles were obtained after 24 h (Figure 4C and D), which can be attributed to an increase in the number of internalized particles and the time required for particles to traffic to the lysosomes. The exposure of particles in the presence or absence of EGF did not change the colocalization values between the particles and lysosomes. The internalization of 130 nm SiO_2 particles might occur through the same endocytic mechanisms as EGFR, as previously stated.

The particles' colocalization with EGFR does not allow for a direct link between particle internalization and EGFR, but it does help to understand whether they have similar intracellular trafficking. The results reveal a weak and a very weak association between particles and EGFR at 6 h for 130 nm and 1 µm particles, respectively (Figure 4E and F). Similarly, to the observations with lysosomes, colocalization values between particles and EGFR increased after 24 h. Interestingly, the presence of EGF increased the colocalization values between the smaller particles and EGFR (Figure 4G). The opposite was observed for the larger particles, where the presence of EGF reduced colocalization values (Figure 4H). EGF stimulation leads to the internalization of EGFR followed by recycling and/or degradation. The increased colocalization values can be associated with the activation of endocytic mechanisms by EGF, which causes internalization of EGFR along with smaller SiO_2 particles. Colocalization is expected to decrease when larger particles are combined with EGF, as larger particles cannot be internalized through the same mechanisms.

Influence of SiO_2 Particles and Epidermal Growth Factor on Migration of Lung Epithelial Cells

Epidermal growth factor is known to influence not only cell proliferation, but also cell migration and invasion.[39] To investigate the effect of EGF and SiO_2 particles on cell migration, a cell migration assay was performed for 24 h (Figure 5D and E). After 6 hours, an increase in cell migration in the presence of EGF and EGF with 1 µm particles is shown. This increase, however, is not observed after 6 h of EGF exposure in the presence of 130 nm particles. Wound confluence is close to 100% after 24 h in all conditions where cells were stimulated with EGF. Untreated cells and cells treated with particles, on the other hand, revealed a wound confluence of 50%. Interestingly, despite the presence of a KRAS mutation[40] in A549 cells, EGF did not affect cell mitochondrial activity but strongly stimulated cell migration.

Influence of SiO_2 Particles and Epidermal Growth Factor on Epidermal Growth Factor Receptor Expression and Extracellular Signal-Regulated Kinases 1/2

To understand the possible effects of SiO_2 particles on the EGFR pathway, the changes in EGFR expression and signaling were investigated. The expression of EGFR and its downstream effectors ERK1/2 (total and phosphorylated) were examined by Western blot after cells' exposure to EGF and SiO_2 particles. After 1 h of exposure to EGF and particles, EGFR expression was not significantly altered (Figure 6A). The endogenous total EGFR levels were decreased in the presence of EGF at 24 h but increased in the presence of both SiO_2 particles (Figure 6B). EGFR protein levels are expected to decrease when stimulated with a high concentration of EGF since a negative feedback mechanism controls and attenuates the extent of downstream signaling, resulting in an increase in EGFR degradation.[41]

Since the particles affected EGFR expression, additional experiments were carried out to evaluate if other components of this signaling pathway were also affected. The downstream signaling pathway ERK/MAPK (RAS/RAF/MEK/ERK) is one of the most important pathways in mediating the EGFR's biological response.[2] The total levels of endogenous ERK1/2 kinase and its activity (phosphorylated form) was evaluated at 1 h, 6 h and 24 h (Figure 7).

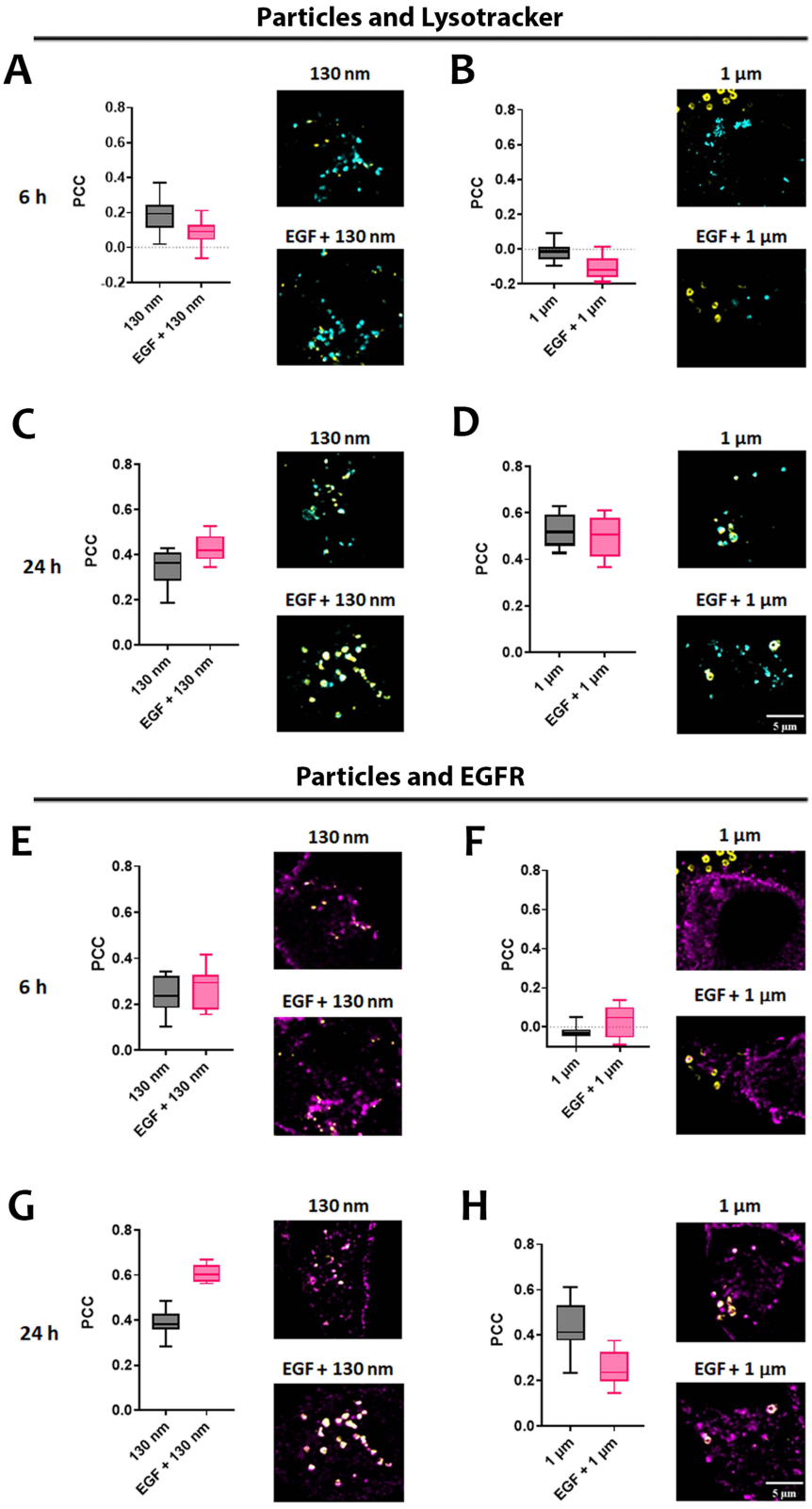

Figure 4 Intracellular localization of SiO_2 particles in lung epithelial cells (A549). Colocalization of SiO_2 particles (yellow) with lysotracker (cyan) at 6 h (**A** and **B**) and 24 h (**C** and **D**) in A549 cells. Colocalization of SiO_2 particles (yellow) with EGFR (magenta) at 6 h (**E** and **F**) and 24 h (**G** and **H**). Pearson correlation coefficient (PCC) values are represented in the box and whiskers graphs. Data are presented as mean ± standard error of mean of 10 individual cells. Representative images of a cell region are shown. Scale bar = 5 µm.

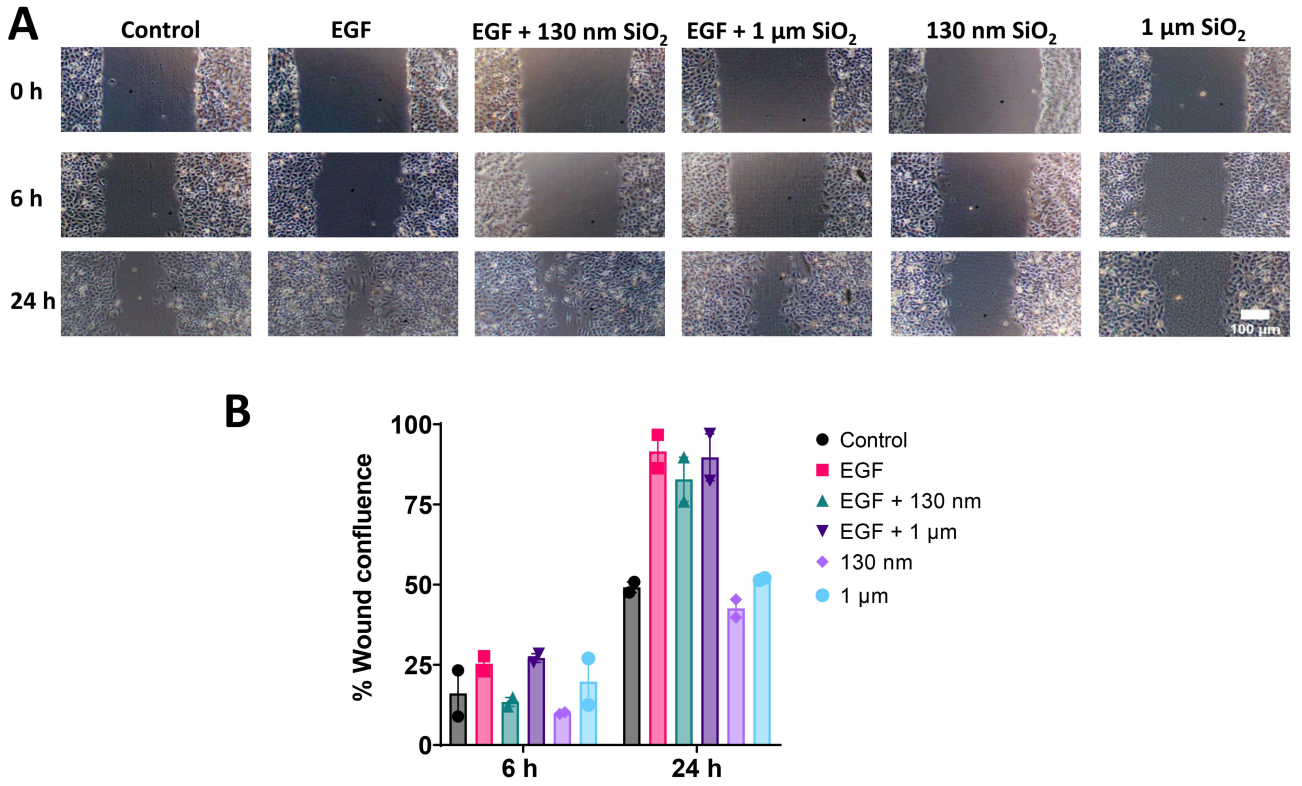

Figure 5 Effect of SiO_2 particles and epidermal growth factor (EGF) on lung epithelial cells (A549) migration. (**A**) Pictures of A549 cells at 0 h, 6 h and 24 h revealing the increased cell migration in the presence of EGF. Scale bar = 100 µm. (**B**) Bar graphs represent the % wound confluence normalized to t = 0 h. Data are presented as mean ± standard error of mean (n = 2).

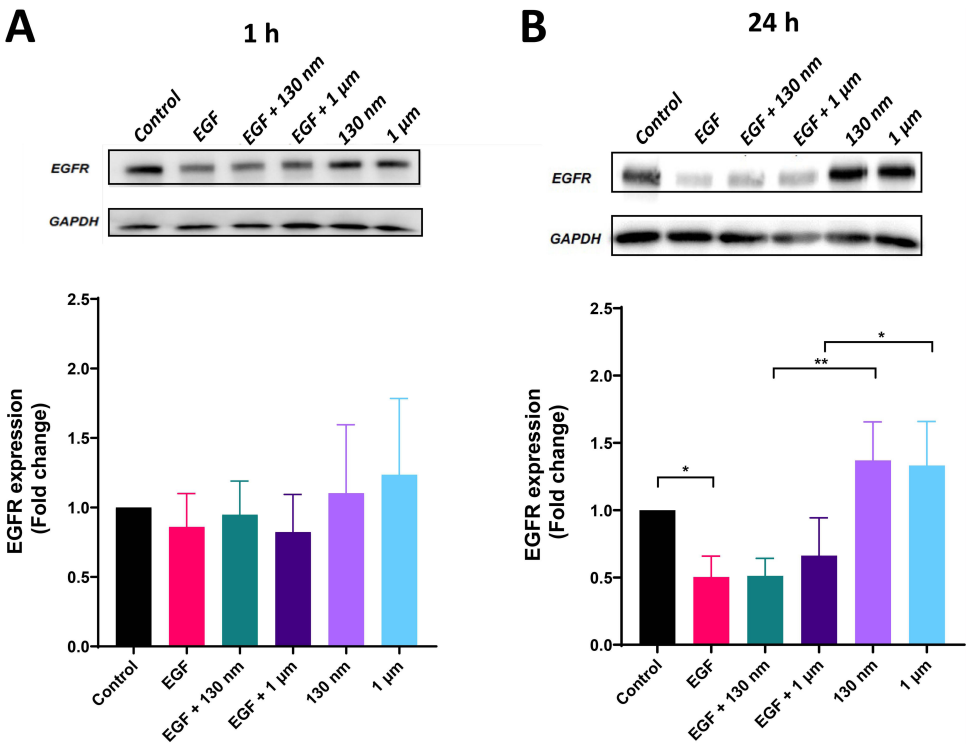

Figure 6 Effect of SiO_2 particles and epidermal growth factor (EGF) on EGFR expression. EGFR expression was determined by Western blot after lung epithelial cells (A549) were exposed to SiO_2 particles and EGF for 1 h (**A**) and 24 h (**B**). Representative Western blot images are shown at the top. Bar graphs, at the bottom, represent the relative EGFR expression upon normalization against the loading control GAPDH. Data are presented as mean ± standard error of mean (n = 4). Statistically significant differences among the groups (One-way ANOVA Tukey's post-hoc test for multiple comparisons): *p ≤ 0.05; **p ≤ 0.01.

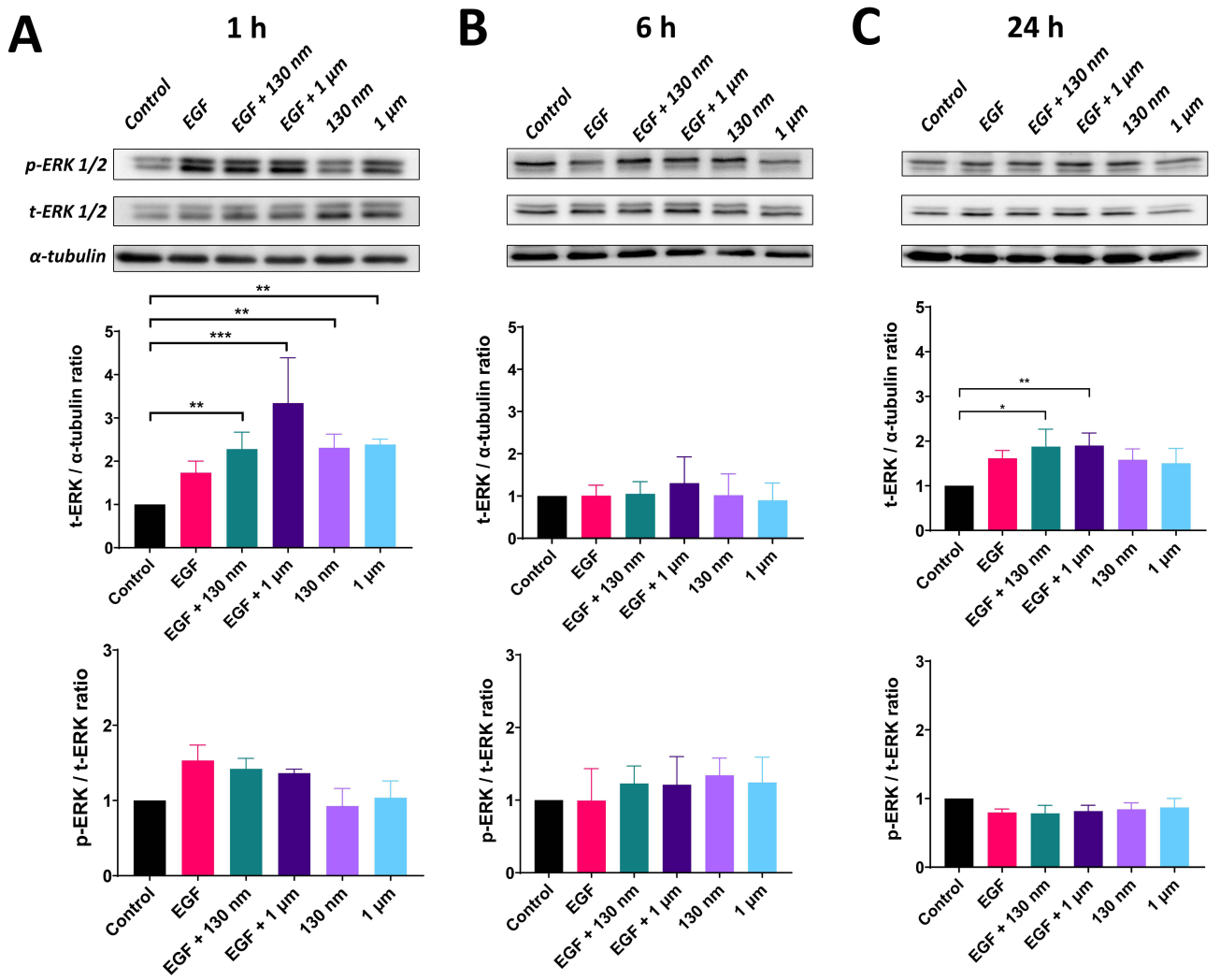

Figure 7 Effect of SiO_2 particles and epidermal growth factor (EGF) on the endogenous levels of ERK1/2 kinase and its activation. The total and phosphorylated protein levels of ERK1/2 were determined by Western blot after lung epithelial cells (A549) were exposed to SiO_2 particles and EGF for 1 h (**A**), 6 h (**B**) and 24 h (**C**). Representative Western blot images are shown at the top. The first bar graph, below the images, represents the relative total ERK1/2 (t-ERK) expression upon normalization against the loading control α-tubulin. The last bar graph, below the first bar graph, represents the relative phosphorylated ERK1/2 (p-ERK1/2) upon normalization against the relative total ERK1/2 and the loading control α-tubulin. The data are presented as mean ± standard error of mean (n = 3). Statistically significant differences among the groups (One-way ANOVA Tukey's post-hoc test for multiple comparisons: *p ≤ 0.05; **p ≤ 0.01; ***p ≤ 0.001; n = 3).

A higher level of total ERK1/2 was observed upon 1 h exposure to SiO_2 particles in the presence and absence of EGF (Figure 7A). Even if not statistically significant, an increase in phosphorylation levels was detected when cells were stimulated with EGF. At 6 h, no significant difference in total or phosphorylated ERK1/2 was observed (Figure 7B). However, a significant rise on the levels of total ERK1/2 was seen at 24 h upon A549 cell exposure to both particles in the presence of EGF (Figure 7C).

The results show that SiO_2 particles interfere with EGFR signaling pathway by increasing EGFR expression and endogenous levels of total ERK1/2 kinase, but without affecting ERK1/2 activity (Figure 8). Kim et al[33] and Wittig et al[34] also observed the activation of the ERK1/2 pathway and increase in ERK1/2 endogenous levels followed by an increase in cell proliferation in hADSC and human gastric carcinoma cells, respectively, after incubation with SiO_2 NPs. In this study, no ERK1/2 activation was observed after SiO_2 particle exposure, which can be attributed to the different particle sizes and time points used. Furthermore, the A549 cell line used in this study has a KRAS mutation, which causes constant activation of the ERK/MAPK pathway independent of ligand binding and may explain the lack of ERK1/2 activation. Additional research using different cell lines and/or primary cells will be necessary to thoroughly understand these findings.

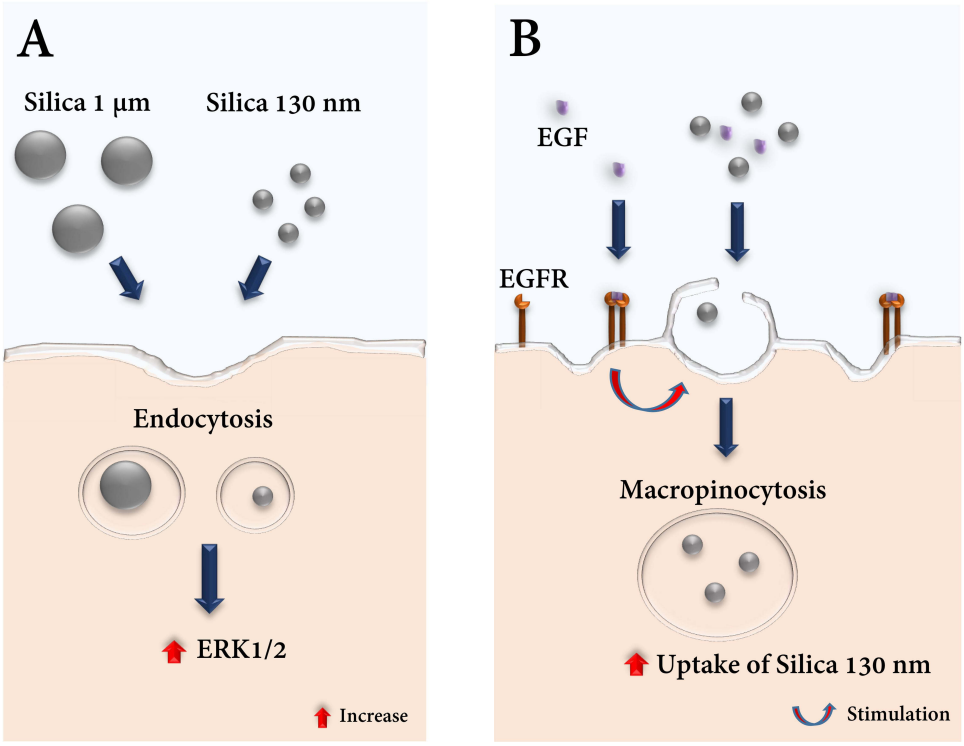

Figure 8 Scheme with proposed molecular mechanisms affected by cellular uptake of silica (SiO_2) particles in the presence or absence of epidermal growth factor (EGF). (**A**) Internalization of both SiO_2 particles via endocytosis increases endogenous levels of ERK1/2. (**B**) The addition of EGF increases the uptake of 130 nm SiO_2 but not 1 µm SiO_2 particles via macropinocytosis.

Conclusions

In the present study, we demonstrated that lung epithelial cells can internalize SiO_2 particles with core diameters of 130 nm and 1 µm after 6 h of exposure and that the particles undergo intracellular trafficking to lysosomes within 24 h. Furthermore, these particles are non-cytotoxic and have no significant effect on cell proliferation and migration. Nevertheless, SiO_2 particles interfere with EGFR signaling pathway by increasing the endogenous levels of ERK1/2 kinase. In contrast to what has been shown in other cell lines,[33,34,42] no influence on ERK1/2 kinase activity was observed.

Furthermore, the addition of the ligand EGF affected SiO_2 particle uptake in a size-dependent manner. The increased uptake of 130 nm SiO_2 particles after 6 h and 24 h is primarily associated with an increase in macropinocytosis induced by EGF. Other mechanisms, such as clathrin and clathrin-independent endocytosis, may also play a role in this outcome. To summarize, particles, both alone and in combination with the ligand EGF, interfere with the EGFR signaling pathway.

The current study reveals that uptake of SiO_2 particles can interfere with cellular signaling pathways and be increased by concomitant exposure with the bioactive molecule EGF. A dose-dependency study of EGF and other growth factors on different cell lines and their effect on NP uptake would help understand the influence of these molecules on the delivery of nanomedicines. The effects of particles per se on biological systems should be considered before moving on specific applications (e.g., functionalization). In nanomedicine, the possibility of combining therapy with bioactive molecules like EGF should be considered to increase the cellular particle dose. This has the potential to improve NP delivery per cell. To facilitate their subsequent approval, the design and development of new (nano)particles for diagnosis and therapy (i.e., theranostics) should remain simple and efficient.

Data Sharing Statement

The datasets underlying the results discussed in this article can be found in the online repository Zenodo under the doi 10.5281/zenodo.7535398 (Accessed on 13 January 2023).

Acknowledgments

The authors would like to thank Laetitia Haeni and Liliane Ackermann Hirschi for their assistance with cell culture, biological assays, and particle synthesis.

Funding

This study was supported by the Swiss National Science Foundation through the National Center of Competence in Research Bio-Inspired Materials (Grant number 51NF40-182881) and the Adolphe Merkle Foundation.

Disclosure

The authors report no conflicts of interest in this work.

References

1. Herbst RS. Review of epidermal growth factor receptor biology. *Int J Radiat Oncol*. 2004;59(2):S21–S26. doi:10.1016/j.ijrobp.2003.11.041
2. Wee P, Wang Z. Epidermal growth factor receptor cell proliferation signaling pathways. *Cancers*. 2017;9(5):52. doi:10.3390/cancers9050052
3. Capuani F, Conte A, Argenzio E, et al. Quantitative analysis reveals how EGFR activation and downregulation are coupled in normal but not in cancer cells. *Nat Commun*. 2015;6(1):7999. doi:10.1038/ncomms8999
4. Pinilla-Macua I, Grassart A, Duvvuri U, Watkins SC, Sorkin A. EGF receptor signaling, phosphorylation, ubiquitylation and endocytosis in tumors in vivo. *Elife*. 2017;6. doi:10.7554/eLife.31993
5. Roepstorff K, Grandal MV, Henriksen L, et al. Differential effects of EGFR ligands on endocytic sorting of the receptor. *Traffic*. 2009;10 (8):1115–1127. doi:10.1111/j.1600-0854.2009.00943.x
6. Freed DM, Bessman NJ, Kiyatkin A, et al. EGFR ligands differentially stabilize receptor dimers to specify signaling kinetics. *Cell*. 2017;171 (3):683–695.e18. doi:10.1016/j.cell.2017.09.017
7. Madshus IH, Stang E. Internalization and intracellular sorting of the EGF receptor: a model for understanding the mechanisms of receptor trafficking. *J Cell Sci*. 2009;122(19):3433–3439. doi:10.1242/jcs.050260
8. Sigismund S, Avanzato D, Lanzetti L. Emerging functions of the EGFR in cancer. *Mol Oncol*. 2018;12(1):3–20. doi:10.1002/1878-0261.12155
9. Harms BD, Bassi GM, Horwitz AR, Lauffenburger DA. Directional persistence of EGF-induced cell migration is associated with stabilization of lamellipodial protrusions. *Biophys J*. 2005;88(2):1479–1488. doi:10.1529/biophysj.104.047365
10. Price JT, Tiganis T, Agarwal A, Djakiew D, Thompson EW. Epidermal growth factor promotes MDA-MB-231 breast cancer cell migration through a phosphatidylinositol 3'-kinase and phospholipase C-dependent mechanism. *Cancer Res*. 1999;59(21):5475–5478.
11. Yamaguchi H, Wyckoff J, Condeelis J. Cell migration in tumors. *Curr Opin Cell Biol*. 2005;17(5):559–564. doi:10.1016/j.ceb.2005.08.002
12. Master AM, Sen Gupta A. EGF receptor-targeted nanocarriers for enhanced cancer treatment. *Nanomedicine*. 2012;7(12):1895–1906. doi:10.2217/nnm.12.160
13. Zhao J, Stenzel MH. Entry of nanoparticles into cells: the importance of nanoparticle properties. *Polym Chem*. 2018;9(3):259–272. doi:10.1039/C7PY01603D
14. Doane TL, Burda C. The unique role of nanoparticles in nanomedicine: imaging, drug delivery and therapy. *Chem Soc Rev*. 2012;41(7):2885. doi:10.1039/c2cs15260f
15. Liberman A, Mendez N, Trogler WC, Kummel AC. Synthesis and surface functionalization of silica nanoparticles for nanomedicine. *Surf Sci Rep*. 2014;69(2–3):132–158. doi:10.1016/j.surfrep.2014.07.001
16. da Santos ES, Nogueira KAB, Fernandes LCC, et al. EGFR targeting for cancer therapy: pharmacology and immunoconjugates with drugs and nanoparticles. *Int J Pharm*. 2021;592:120082. doi:10.1016/j.ijpharm.2020.120082
17. Silva CO, Petersen SB, Reis CP, et al. EGF functionalized polymer-coated gold nanoparticles promote EGF photostability and EGFR internalization for photothermal therapy. Antopolsky M, ed. *PLoS One*. 2016;11(10):e0165419. doi:10.1371/journal.pone.0165419
18. She X, Chen L, Velleman L, et al. The control of epidermal growth factor grafted on mesoporous silica nanoparticles for targeted delivery. *J Mater Chem B*. 2015;3(29):6094–6104. doi:10.1039/C5TB00790A
19. Corbo C, Molinaro R, Parodi A, Toledano Furman NE, Salvatore F, Tasciotti E. The impact of nanoparticle protein corona on cytotoxicity, immunotoxicity and target drug delivery. *Nanomedicine*. 2016;11(1):81–100. doi:10.2217/nnm.15.188
20. Monopoli MP, Walczyk D, Campbell A, et al. Physical−chemical aspects of protein corona: relevance to in vitro and in vivo biological impacts of nanoparticles. *J Am Chem Soc*. 2011;133(8):2525–2534. doi:10.1021/ja107583h
21. Sousa de Almeida M, Susnik E, Drasler B, Taladriz-Blanco P, Petri-Fink A, Rothen-Rutishauser B. Understanding nanoparticle endocytosis to improve targeting strategies in nanomedicine. *Chem Soc Rev*. 2021;7:2885–2911. doi:10.1039/d0cs01127d
22. Ma L, Kohli M, Smith A. Nanoparticles for combination drug therapy. *ACS Nano*. 2013;7(11):9518–9525. doi:10.1021/nn405674m
23. Phuc L, Taniguchi A. Epidermal growth factor enhances cellular uptake of polystyrene nanoparticles by clathrin-mediated endocytosis. *Int J Mol Sci*. 2017;18(6):1301. doi:10.3390/ijms18061301
24. Stöber W, Fink A, Bohn E. Controlled growth of monodisperse silica spheres in the micron size range. *J Colloid Interface Sci*. 1968;26(1):62–69. doi:10.1016/0021-9797(68)90272-5
25. Larson DR, Ow H, Vishwasrao HD, Heikal AA, Wiesner U, Webb WW. Silica nanoparticle architecture determines radiative properties of encapsulated fluorophores. *Chem Mater*. 2008;20(8):2677–2684. doi:10.1021/cm7026866
26. Crippa F, Rodriguez-Lorenzo L, Hua X, et al. Phase transformation of superparamagnetic iron oxide nanoparticles via thermal annealing: implications for hyperthermia applications. *ACS Appl Nano Mater*. 2019;2(7):4462–4470. doi:10.1021/acsanm.9b00823

27. Fong W-K-K, Moore TL, Balog S, et al. Nanoparticle behaviour in complex media: methods for characterizing physicochemical properties, evaluating protein corona formation, and implications for biological studies. In: *NanoScience and Technology*. Springer;2019:101–150. doi:10.1007/978-3-030-12461-8_5
28. Stauffer W, Sheng H, Lim HN. EzColocalization: an ImageJ plugin for visualizing and measuring colocalization in cells and organisms. *Sci Rep*. 2018;8(1). doi:10.1038/s41598-018-33592-8
29. Sousa de Almeida M, Taladriz-Blanco P, Drasler B, et al. Cellular uptake of silica and gold nanoparticles induces early activation of nuclear receptor NR4A1. *Nanomaterials*. 2022;12(4):690. doi:10.3390/nano12040690
30. Moore TL, Rodriguez-Lorenzo L, Hirsch V, et al. Nanoparticle colloidal stability in cell culture media and impact on cellular interactions. *Chem Soc Rev*. 2015;44(17):6287–6305. doi:10.1039/C4CS00487F
31. Shapero K, Fenaroli F, Lynch I, Cottell DC, Salvati A, Dawson KA. Time and space resolved uptake study of silica nanoparticles by human cells. *Mol BioSyst*. 2011;7(2):371–378. doi:10.1039/C0MB00109K
32. Uboldi C, Bonacchi D, Lorenzi G, et al. Gold nanoparticles induce cytotoxicity in the alveolar type-II cell lines A549 and NCIH441. *Part Fibre Toxicol*. 2009;6(1):18. doi:10.1186/1743-8977-6-18
33. Kim KJ, Kim MK, Rhie JW, et al. Silica nanoparticles increase human adipose tissue-derived stem cell proliferation through ERK1/2 activation. *Int J Nanomedicine*. 2015:2261. doi:10.2147/IJN.S71925
34. Wittig A, Gehrke H, Del Favero G, et al. Amorphous silica particles relevant in food industry influence cellular growth and associated signaling pathways in human gastric carcinoma cells. *Nanomaterials*. 2017;7(1):18. doi:10.3390/nano7010018
35. Behzadi S, Serpooshan V, Tao W, et al. Cellular uptake of nanoparticles: journey inside the cell. *Chem Soc Rev*. 2017;46(14):4218–4244. doi:10.1039/C6CS00636A
36. Gustafson HH, Holt-Casper D, Grainger DW, Ghandehari H. Nanoparticle uptake: the phagocyte problem. *Nano Today*. 2015;10(4):487–510. doi:10.1016/j.nantod.2015.06.006
37. Guo X, Huang L. Recent advances in non-viral vectors for gene delivery. *Acc Chem Res*. 2013;45(7):971–979. doi:10.1021/ar200151m.Recent
38. Nakase I, Kobayashi NB, Takatani-Nakase T, Yoshida T. Active macropinocytosis induction by stimulation of epidermal growth factor receptor and oncogenic ras expression potentiates cellular uptake efficacy of exosomes. *Sci Rep*. 2015;5(1):10300. doi:10.1038/srep10300
39. Schelch K, Vogel L, Schneller A, et al. EGF induces migration independent of EMT or invasion in A549 lung adenocarcinoma cells. *Front Cell Dev Biol*. 2021;9. doi:10.3389/fcell.2021.634371
40. Yoon Y-K, Kim H-P, Han S-W, et al. KRAS mutant lung cancer cells are differentially responsive to MEK inhibitor due to AKT or STAT3 activation: implication for combinatorial approach. *Mol Carcinog*. 2010;49(4):353–362. doi:10.1002/mc.20607
41. Tanaka T, Zhou Y, Ozawa T, et al. Ligand-activated epidermal growth factor receptor (EGFR) signaling governs endocytic trafficking of unliganded receptor monomers by non-canonical phosphorylation. *J Biol Chem*. 2018;293(7):2288–2301. doi:10.1074/jbc.M117.811299
42. Gehrke H, Frühmesser A, Pelka J, et al. In vitro toxicity of amorphous silica nanoparticles in human colon carcinoma cells. *Nanotoxicology*. 2012;7(3):274–293. doi:10.3109/17435390.2011.652207